Optica Applicata, Vol. XXVI, No 3, 1996

A physics-based approach to identifying interreflection

TARDI TJAHJADI

Department of Engineering, University of Warwick, Coventry CV4 7AL, United Kingdom.

D. LITWIN

Institute of Applied Optics, ul. Kamionkowska 18, 03–805 Warszawa, Poland.

YEE-HONG YANG

Department of Computer Science, University of Saskatchewan, 57 Campus Drive, Saskatoon, Saskatchewan, Canada S7N 5A9.

A reflection model which enables an identification of matte, highlight and interreflection regions on objects of inhomogeneous dielectric materials is presented. The model utilises the concept of the dichromatic reflection model and the one-bounce model of mutual reflection. A $\varphi-\theta$ space is introduced to enable the spectral cluster of a region to be identified either as a matte hill, a highlight lobe or an interreflection lobe. An analysis of the boundary of clusters enables the use of the K-means clustering algorithm to segment the regions without the need to specify the expected number of clusters and the initial cluster centres.

1. Introduction

Interreflection occurs when light reflected from one surface impinges on another surface. It alters the hue and brightness of the affected pixels in colour images. Unaccounted for interreflection can easily confuse image processing algorithms because interreflection alters image grey levels in a consistent, non-random way so that any errors it introduces, say, a shape-from-shading solution accumulate rather than cancel out [1].

For the most accurate available model, light-matter interaction can be described in terms of the interaction of photons with atoms or molecules [2]. However, it would be a formidable task to derive image processing algorithms from a physical model at such a low level. Therefore, it is often necessary to sacrifice some degree of physical accuracy in order to obtain a useful model.

Materials can be classified into two classes on the basis of their optical properties [3]. Optically homogeneous materials, *e.g.*, metals, glass and crystals, have a constant index of refraction throughout the material. Therefore light undergoes reflection and refraction only as it encounters an object surface, *i.e.*, there is only interface or surface reflection. Optically inhomogeneous materials, *e.g.*, ceramics,

plastics and paper, consist of a medium and some embedded pigments. By assuming that the pigments are completely embedded in the medium and the Fresnel coefficients of the medium are constant over the visible spectrum, the surface component has approximately the same spectral power distributions as the illumination [4], [5]. For typical objects with rough surfaces, the surface reflection is diffused around the direction of perfect specular reflection [6]. By assuming that the pigments are distributed randomly in the body, the light that is reflected from the material body has the same colour over the entire surface. The body reflection component thus provides the characteristic object colour and is modulated by shading.

A method for recovering the shape and surface reflectance of a scene in the presence of interreflection uses an iterative scheme in which an estimate of the shape is calculated from the intensity data, and the radiosity method is used to estimate the no-interreflection image until convergence [7]. However, it has only been applied to white interreflecting surfaces and does not take into account the colour of the interreflected light.

The one-bounce model of mutual reflection utilises the fact that the intensity of interreflection diminishes substantially with each bounce [8]. It provides an accurate description of mutual reflection between two matte, convex Lambertian surfaces each of uniform colour, with an illumination that can vary spatially in its intensity but not in its spectral composition. FUNT and DREW [1] show that the singular value decomposition of colours emanating from a surface lie on a plane in the RGB colour space. The intersection of two planes which correspond to the two regions of interreflection, one on each of the interreflecting surfaces, determines the colour of the interreflected light. This algorithm assumes that the two regions of interreflection have been segmented.

This paper proposes a new reflection model which is based on the dichromatic reflection model [3], [9], and utilises the concept of the one-bounce model for the analysis of interreflection in colour images. The model enables regions of interreflection on an object of inhomogeneous dielectric materials to be differentiated from regions of matte reflection and highlight. The paper also introduces a $\varphi - \theta$ colour space so as to enable an automatic segmentation of regions of interreflection, of matte reflection and of highlight.

2. Image modelling

The dichromatic reflection model [3], [9] describes light reflection by inhomogeneous dielectric materials, *e.g.*, ceramics and plastics, as a sum of that reflected at the surface interface and that by the material body, and scaled by the geometric reflection properties. The surface reflection component has approximately the same spectral power distribution as the illumination and appears predominantly as a highlight on the object. The body reflection component provides the characteristic object colour and is modulated by shading. It appears predominantly as the matte areas on the object.

The model states that the light spectra of the body reflection and surface re-

flection are constant over an entire object, while the geometric scale factors vary with the illumination and viewing angles [9]. The light spectra from an object form a dense spectral cluster in the dichromatic plane in the RGB colour space. The shape of this cluster is related to the shape of the object. For matte object points, the surface reflection is negligible, and therefore the observed light depends only on the light spectra of the body reflection, and scaled according to the geometrical relationship between the local surface normal of the object and the viewing and illumination directions. Consequently the light reflected from the matte object points forms a linear cluster (referred to as a matte line) in the direction of the light spectra of the body reflection. For highlight object points, the body reflection component is approximately constant and the spectral variation is due to the geometry of the scene. Consequently the light reflected from the highlight object points forms a linear cluster (referred to as a highlight line) from some position along the matte line, and in the direction of the light spectra of the surface reflection.

For an object with convex surface, *e.g.*, a cylindrical object, and illuminated by a light source whose colour is different from that of the object, the two reflection components form a skewed T-shaped spectral cluster consisting of a matte and a highlight line. The skewing angle depends on the spectral difference between the body and the surface reflection, while the position of the highlight line depends on the illumination geometry. In the case of a concave object, *e.g.*, an object with two surfaces inclined at an obtuse angle, the illuminant (of a different colour to the object) creates a highlight on each of the surfaces. Therefore the spectral cluster of this object consists of two highlight lines which are parallel to one another, and emanating from two positions along a matte line [9].

The dichromatic reflection model has been shown, using the Reichmann body-scattering model, to be a reasonable approximation [10]. The applicability of the reflection model can be extended to include homogeneous materials by considering only surface reflection, the unichromatic reflection model, which has been shown using the Torrance–Sparrow surface reflection model and the Fresnel equations to be a reasonable approximation for metals [10]. The reflection model allows the physical attributes of surfaces to be taken into account and acts as a priori knowledge for colour image analysis.

2.1. Function-based approach to image modelling

We model a colour image by considering how light is attenuated and altered by the absorption of a range of wavelengths as it is reflected from various points on an object surface. This leads to the concept of describing a surface as a function of colour and spatial position, *i.e.*, $F: \Psi \times \Psi \times A \rightarrow \Psi$, where Ψ is the set of wavelengths used to describe the colour of the light, and A is a set whose elements define spatial information. Thus $F(\psi_S, \psi_I, \alpha)$ is the reflected light from a surface with ψ_S denoting the colour of the surface, ψ_I – the colour of the incident illumination and α – the spatial information. F itself is a function which is defined for the physical properties of the surface.

From the ideas of superposition of waves, and the continuously variant nature of wavelengths in light, light can be considered as an infinite dimensional vector space, with any one colour described as the combination of some of its component wavelengths, and intensity as the value of some metric on the space. To simplify matters when considering the output of a colour camera, only the three primary wavelengths are taken into account. All other wavelengths may be considered to be attenuated to zero. This reduces the continuous infinite dimensional case into a discrete three dimensional. Further, the concept of colour and intensity can be combined in the three dimensional vector $\vec{\lambda} = (\lambda_R, \lambda_G, \lambda_B)$ which measures the intensity of each of the primary wavelengths present, and for the purpose of normalisation the values of the λ's are considered to be in the range $[0,1]$. It now becomes possible to define *colour* as the unit vector $\hat{\lambda}$ and the *intensity* as the Euclidean length of the vector.

By treating light as a vector, a pixel can be considered to have several colour components, each possibly caused by a different physical effect, that combine together, summing to form the overall colour of the pixel. If each point on the surface of a dielectric object is considered to be the summation of a matte reflection component and a specular highlight component, where the relative scalings of these vector quantities are determined by its spatial position, then according to the dichromatic reflection model the colour of a pixel in the image space is

$$L(\lambda_S, \lambda_I, \alpha) = C_B(\alpha) B(\lambda_S, \lambda_I) + C_S(\alpha) S(\lambda_S, \lambda_I) \tag{1}$$

where: $L: \Lambda \times \Lambda \times A \to \Lambda, \alpha \in A$ is the geometric factor, $\lambda_S \in \Lambda$ is the colour of the surface, and $\lambda_I \in \Lambda$ is the colour of the incident illumination. $C_B(\alpha)$ and $C_S(\alpha)$ are the proportions of body and specular reflection in the colour $L(\lambda_S, \lambda_I, \alpha)$, respectively, and $B: \Lambda \times \Lambda \to \Lambda$ and $S: \Lambda \times \Lambda \to \Lambda$ are functions returning the colour of the body and specular reflections.

Various spectral clusters are formed when the colours of all the pixels are plotted in the RGB colour space. The shape of each of these clusters can be used to provide a priori information about the object surfaces. Since this grouping of colour points is independent of the geometric information, Eq. (1) can be rewritten as

$$L(\lambda_S, \lambda_I) = C_B B(\lambda_S, \lambda_I) + C_S S(\lambda_S, \lambda_I). \tag{2}$$

The spectral cluster of the entire surface thus lies somewhere within the parallelogram defined by the two vectors $B(\lambda_S, \lambda_I)$ and $S(\lambda_S, \lambda_I)$. Since C_B changes slowly compared to C_S, a useful simplification is to consider C_B as constant and C_S as variable. The spectral cluster of a convex dielectric surface on a black background consists of two linear clusters. The first cluster, the matte line, is approximately a straight line that starts at the origin of the RGB space and extends in the direction of $B(\lambda_S, \lambda_I)$. The second cluster, the highlight line, starts at some point along the matte line and extends in the direction of $S(\lambda_S, \lambda_I)$.

2.2. Modified dichromatic reflection model

When considering the possible physical effects and interactions among surfaces, treating a surface as a function allows the light radiated by one surface to be acted on by another. Thus,

$$L = C_B B(\lambda_S, C_S^1 S(\lambda_S^1, \lambda_I)) \tag{3}$$

is the matte reflective effect of the surface reflection from surface S^1 onto the primary surface S. A model that incorporates reflective effects from a number of adjacent surfaces on a surface is

$$L = C_B B(\lambda_S, \lambda_I) + C_S S(\lambda_S, \lambda_I) + \sum_{i \in \Omega} \{C_B B(\lambda_S, C_B^i B(\lambda_S^i, \lambda_I)) + C_B B(\lambda_S, C_S^i S(\lambda_S^i, \lambda_I)) + C_S S(\lambda_S, C_B^i B(\lambda_S^i, \lambda_I)) + C_S S(\lambda_S, C_S^i S(\lambda_S^i, \lambda_I))\} \tag{4}$$

where Ω is a set of surfaces S_i that might affect S.

Equation (4) can be simplified using observed physical properties. The first property is that the specular highlight from a dielectric surface is approximately the same colour as the incident illumination, thus the function of surface reflection, $S: \Lambda \times \Lambda \to \Lambda$, may be considered as merely an attenuation of the incident light

$$\forall \lambda_S, \lambda_I \in \Lambda, \quad S(\lambda_S, \lambda_I) = \Gamma \lambda_I, \text{ with } \Gamma \in \mathscr{R} \tag{5}$$

where $\mathscr{R}$ is the set of real numbers.

Assuming that all wavelengths are absorbed equally in a surface and that temperature change in the surface due to absorption of light energy generates negligible effect, then the function of body reflection may be considered as linear with respect to intensity. This is because a fixed proportion of the light flux will exit the surface, no matter how much or little is applied. This can perhaps be explained by considering the probability of one photon being absorbed or reflected by the surface. This probability is dependent on the path of the photon through the surface and its "collision" with particles of pigment in the object, it is independent of the number of photons passed at any instant. Thus,

$$\forall \beta \in \mathscr{R}^+ \text{ and } \lambda_S, \lambda_I \in \Lambda, \quad B(\lambda_S, \beta \lambda_I) = \beta B(\lambda_S, \lambda_I) \tag{6}$$

where $\mathscr{R}^+$ is the set of positive or zero real numbers.

When a coloured surface is viewed, most of the incident light is absorbed in all but the colour of the surface. However, the incident light itself may also have a colour, and any reflected light from the surface cannot have any of the wavelengths not present in the incident light. Furthermore, no component of the wavelength may be greater in magnitude than it was in the incident light. This leads to a theoretical maximum for the body reflection

$$\forall \lambda_S, \lambda_I \in \Lambda, \quad B(\lambda_S, \lambda_I) \in \overline{\lambda_S} \cap \overline{\lambda_I} \tag{7}$$

where

$$\overline{\lambda} = \{(\alpha_R,\alpha_G,\alpha_B):0 \leqslant \alpha_X \leqslant \lambda_X, \quad \forall X \in \{R,G,B\}\} \tag{8}$$

with $\lambda = (\lambda_R,\lambda_G,\lambda_B)$.

Although any one surface may be visibly affected by an arbitrary number of neighbouring surfaces, when a local region of a surface is considered it is likely that at most one of the neighbouring surfaces will have any effect. This is because only one illuminant is used, and in practice the neighbouring surfaces will be of a size comparable to the local region. Thus Eq. (4) may be restricted to a single adjacent surface for the purpose of local region analysis

$$\begin{aligned} L = {} & C_B B(\lambda_S,\lambda_I) + \Gamma C_S \lambda_I + \{C_B B(\lambda_S, C_B^{adj} B(\lambda_S^{adj},\lambda_I)) + C_B B(\lambda_S, \Gamma^{adj} C_S^{adj} \lambda_I) \\ & + \Gamma C_S C_B^{adj} B(\lambda_S^{adj},\lambda_I) + \Gamma \Gamma^{adj} C_S^{adj} C_S \lambda_I\} \end{aligned} \tag{9}$$

with Γ and Γ^{adj} denoting the scalar attenuation factors for the primary and adjacent surface, respectively, and "adj" denoting the adjacent surface. Assuming that Γ and Γ^{adj} are similar in magnitude and that the body reflection varies linearly with respect to intensity, Eq. (9) can be expressed as

$$\begin{aligned} L = {} & C_B B(\lambda_S,\lambda_I) + \Gamma C_S \lambda_I + C_B B(\lambda_S, C_B^{adj} B(\lambda_S^{adj},\lambda_I)) \\ & + \Gamma C_B C_S^{adj} B(\lambda_S,\lambda_I) + \Gamma C_S C_B^{adj} B(\lambda_S^{adj},\lambda_I) + \Gamma^2 C_S^{adj} C_S \lambda_I \\ = {} & \{(C_B + \Gamma C_B C_S^{adj}) B(\lambda_S,\lambda_I) + \Gamma C_S \lambda_I\} + \Gamma C_S \{C_B^{adj} B(\lambda_S^{adj},\lambda_I) + \Gamma C_S^{adj} \lambda_I\} \\ & + C_B B(\lambda_S, C_B^{adj} B(\lambda_S^{adj},\lambda_I)), \end{aligned} \tag{10}$$

$C_B + \Gamma C_B C_S^{adj}$ can be replaced with another scalar variable C'_B. Furthermore, the additional attenuation caused by the term $B(\lambda_S, C_B^{adj} B(\lambda_S^{adj},\lambda_I))$ renders this term very small, and it is likely that it will have a negligible visual effect. So, the final simplification of the model, *i.e.*, the modified dichromatic reflection model that incorporates interreflection is

$$L = \{C'_B B(\lambda_S,\lambda_I) + \Gamma C_S \lambda_I\} + \Gamma C_S \{C_B^{adj} B(\lambda_S^{adj},\lambda_I) + \Gamma C_S^{adj} \lambda_I\}. \tag{11}$$

The modified dichromatic reflection model has an intuitive physical interpretation. It is the double image of the dichromatic model. There is the feature $C'_B B(\lambda_S,\lambda_I) + \Gamma C_S \lambda_I$ that relates to the distinctive skewed T structure of the original model for convex objects, and an attenuated cluster given by $\Gamma C_S \{C_B^{adj} B(\lambda_S^{adj},\lambda_I) + \Gamma C_S^{adj} \lambda_I\}$. This cluster can be considered as a scaled version of the cluster that is expected when an adjacent surface is viewed. This is because the primary surface spectrally reflects the light incident on it. The range of wavelengths in the reflected light corresponds to another scewed Tcluster. Thus, the primary surface may be viewed as a function on the incident light, and the adjacent surface as a source of low-intensity illumination. The modified dichromatic reflection model indicates the presence of an additional matte cluster which corresponds to the interreflection.

2.3. Verifying the modified dichromatic reflection model

To verify the proposed reflection model, several colour images of a scene each con-

taining a cylindrical ceramic object were grabbed using a JVC TK870E CCD colour camera. The scene was illuminated by a tungsten light which was placed at a distance of about 0.2 metres from the object and at an angle of about 45 degrees from the horizon. The object was single-coloured and was placed near another single-coloured cylindrical object of a different hue to generate a region of interreflection. To simplify the verification process, the second object was not placed in the camera view, both objects were suspended in air about 0.2 metres from a black velvet background to suppress the effect of shadows, and the region of interreflection was sufficiently bright when compared with the background.

Figure 1 (see coloured inserts following page 212) shows an image of a bright green ceramic mug and the interreflection is due to a bright yellow paper cylinder. The spectral clusters of the image, Fig. 2, show a skewed T-shaped spectral cluster (albeit fuzzy) and a smaller cluster near the origin of the RGB colour space.

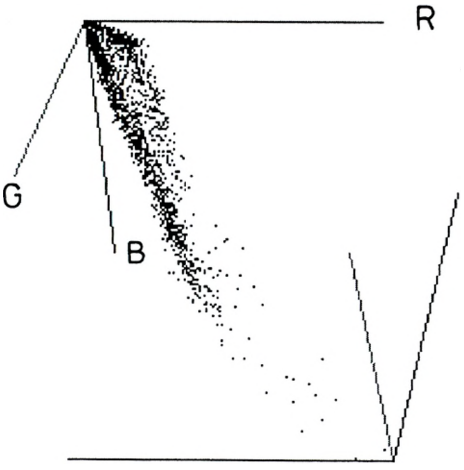

Fig. 2. Spectral clusters of image in Fig. 1

To verify that the smaller cluster corresponds to the region of interreflection, the regions of highlight pixels (*i.e.*, with $R = 255$, $G = 255$ and $B = 255$) and the background pixels (*i.e.*, with $R < 10$, $G < 10$ and $B < 10$) in the image were first segmented and removed using a thresholding process. A K-means clustering algorithm [11] was then applied to the remaining pixels. The clustering process determined two spectral clusters: one corresponding to the matte cluster of the primary object surface; and a smaller cluster which is oriented at an angle to the first, and is located near the origin of the RGB colour space.

The elements of the two clusters were mapped back onto the image, and the results are shown in Fig. 3. The figure shows the matte cluster of the primary object surface as a green region and the smaller cluster as yellow regions, the region of interreflection. The white and black regions correspond to the highlight and background regions, respectively. Comparing Fig. 1 and Fig. 3 (see coloured inserts

following page 212) shows that the various regions are correctly segmented and the experimental results conform to what the modified dichromatic reflection model predicts.

3. $\varphi-\theta$ colour space

The spectral clusters of an image in the RGB colour space, *e.g.*, Fig. 2, do not contain sufficient information to indicate with confidence whether there are any regions of highlight and interreflection. Also, in using the K-means clustering algorithm we need to specify the number of expected clusters and the initial guess of the cluster centres. We therefore introduce the $\varphi-\theta$ colour space (Fig. 4) as a means to identifying the different type of clusters in an image, and determining the initial cluster centres for the clustering algorithm.

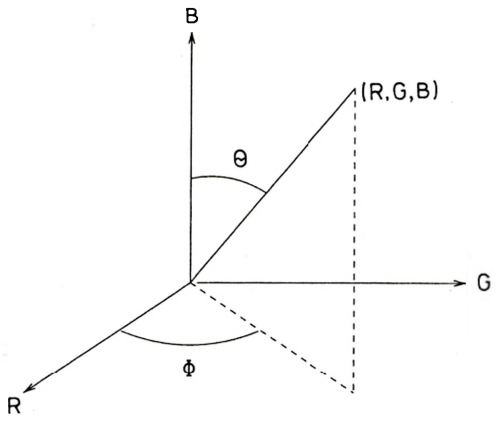

Fig. 4. The $\varphi-\theta$ colour space

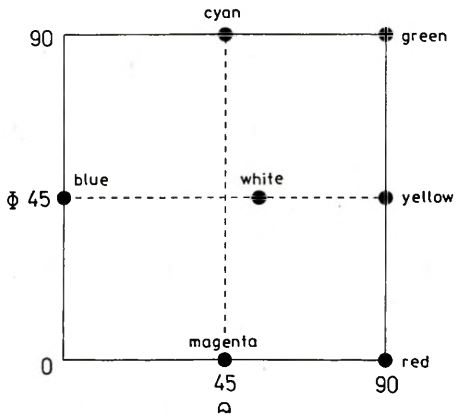

Fig. 5. The $\varphi-\theta$ plane

The $\varphi-\theta$ colour space is obtained from the RGB colour space using the following transformation:

$$\varphi = \arctan\left(\frac{G}{R}\right),$$

$$\theta = \arctan\left(\frac{\sqrt{R^2+G^2}}{B}\right), \tag{12}$$

$$d = \sqrt{R^2+G^2+B^2}$$

where R, G and B are the red, green and blue grey levels of an image pixel, respectively, φ and θ define the direction of the (R, G, B) vector and d represents the intensity of a pixel. Since only the direction of a colour vector is required for the identification of interreflection or object regions, d is dropped. We use φ and θ to represent the normalised RGB vector, and all the image colour points lie on the $\varphi-\theta$ plane (see Fig. 5). The position of the primary and three other colours on this plane are indicated.

Note that R and B may be zero and will cause φ and θ to be undefined. Also, if R and G are very small then a smal variation in R/G causes a large variation in φ. We therefore assume that when $R = G = 0$ and $B \neq 0$, then pure blue is indicated. The table is formulated to deal with these cases.

Table. Special cases to consider when using the $\varphi-\theta$ transformation

R	G	B	φ	θ	Comment
$\neq 0$		$\neq 0$	Eq. (12)	Eq. (12)	All combinations
$\neq 0$	0	0	0	90	Red
0	$\neq 0$	0	90	90	Green
0	0	$\neq 0$	45	0	Blue
$\neq 0$	$\neq 0$	0	Eq. (12)	90	Yellow
0	$\neq 0$	$\neq 0$	90	Eq. (12)	Cyan
0	0	0	0	0	Black

Figure 6 (see coloured inserts following page 212) shows an image of a blue mug, and two paper cylinders, one yellow and one green. Each of the two paper cylinders caused a region of interreflection on the blue mug. The three objects were suspended in air above a black velvet background so that each of the objects can be isolated from each other easily by thresholding. Figure 7 (see coloured inserts following page 212) shows the spectral clusters of the yellow cylinder on the $\varphi-\theta$ plane as a 3-D plot, as a contour plot and as a colour plot. Figures 8 and 9 (see coloured inserts following page 212) show the corresponding spectral clusters of the green cylinder and blue mug, respectively. In the colour plot, the R, G, B values in the image are

normalised as follows:

$$r = \frac{R}{\max[R,G,B]}, \qquad g = \frac{G}{\max[R,G,B]}, \qquad b = \frac{B}{\max[R,G,B]}. \tag{13}$$

This normalisation is only used for enhancing the visualisation of the spectral clusters.

The 3-D plots of Figures 7 and 8 show that when there is no region of interreflection in an object region, the spectral cluster of the object approximates a Gaussian distribution of colours with an extension in the direction of any highlight (also the colour of the illuminant). This extension when viewed as a contour plot and a colour plot appears as an elongated lobe. The Gaussian distribution corresponds to a matte region and is referred to as a matte hill. The lobe corresponds to a highlight region and is referred to as a highlight lobe.

When there are regions of interreflection on an object then the spectral cluster consists of a Gaussian distribution of colours with extensions in the direction of the colour of the objects which cause the interreflection, and any highlight. Figure 9 (see coloured inserts following page 212) shows two lobes which correspond to the two regions of interreflection on the blue mug. These are referred to as interreflection lobes. One of the interreflection lobes also incoroprates a highlight, but this is not a problem because a highlight region can easily be removed by region growing (see Sect. 4). The results are shown in Fig. 10 (see coloured inserts following page 212). Thus the $\varphi - \theta$ colour space reveals that the nature of highlight and interreflection is similar. Regions of interreflection could be treated as the image of an additional light source, the secondary object which causes the interreflection. Note also that the matte hill will have the tallest peak in the spectral cluster. This is because in practice the matte region is normally the largest of the tree types of region within an object. Thus, the $\varphi - \theta$ space provides a simple (*i.e.*, not time-consuming) means of obtaining a priori information about the regions within an object.

Note that if the primary object is very desaturated (*i.e.*, close to white) then the colour of the interreflection region is approximately the same colour as the secondary object which causes the interreflection. Otherwise, if the primary object is saturated, then the tip of the interreflection lobe will not be the colour of the secondary object. For example, if the secondary object is a green cylinder and the primary object is a saturated red plastic cup as shown in Fig. 11**a**, then the colour of the interreflection is yellow as shown by the rightmost lobe of Fig. 11**c**. Figure 11**b** shows the spectral cluster of the green cylinder (see coloured inserts following page 212).

4. Design of the segmentation algorithm

The objective of the segmentation algorithm is to utilise the proposed reflection model and the a priori information about images of inhomogeneous objects to identify/extract the matte region and any regions of highlight and interreflection

within an object region automatically. The segmentation of the image into object and background regions is not of importance in this paper, and therefore this process is facilitated by using a black velvet background, and with the objects not touching one another and suspended in air. In this way the object regions can be extracted simply by thresholding before the segmentation within an object region is undertaken.

From the reflection model we note that an object region consists of a matte and a highlight region. It may also consist of one or more regions of interreflection. From Sect. 3 the spectral cluster of an object will consist of a matte hill and possibly one or more lobes as shown in Fig. 12. Since the matte region is usually the largest of

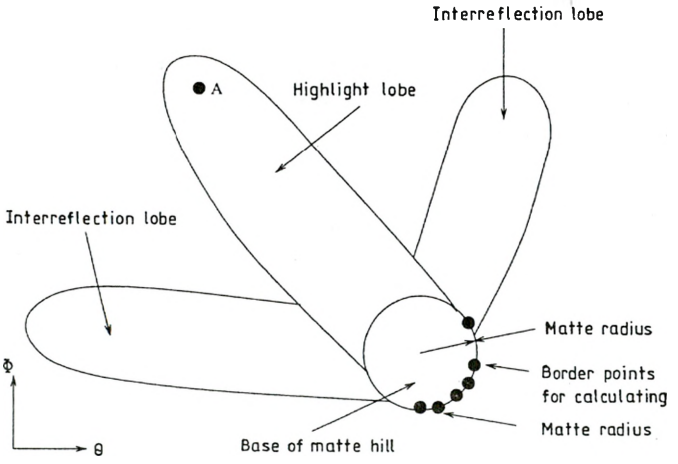

Fig. 12. Expected spectral clusters of an object with two regions of interreflection and a highlight region

the three types of regions, a search is made to locate the tallest peak in the spectral cluster. This peak will correspond to approximately the centre of a matte hill, referred to as the matte centre. The approximate radius of the base of the matte hill is then computed by taking the average of the 14 border points (as indicated in Fig. 12) with the shortest distance from the matte centre. Points within a circle of this radius are considered as matte image pixels, without any highlight or interreflection.

In this paper, a border point refers to a point on the boundary of the base of the spectral cluster plot of an image, *i.e.*, the outermost contour of the contour plot of a spectral cluster (*e.g.*, Fig. 10). It should have at least one neighbouring spectral point and one neighbouring non-spectral point in a 3×3 neighbourhood.

A lobe may not be connected to the rest of the spectral cluster of an object as a result of very few points between the matte centre and the tip of the lobe, or because of noise. This will result in more than one boundary. In this situation the boundary with the greatest number of border points is chosen to be the one which surrounds the matte peak.

As noted in Figures 9 and 10 a highlight lobe may be part of an interreflection lobe. Therefore, it is essential to remove highlight pixels because they distort the

shape of the interreflection lobe. Since highlight pixels are situated in the bright area of an object region whereas interreflections are located in the shadowed part of the object region, they are spatially separated. Therefore highlight pixels are removed (and hence segmented) by applying a region growing process from the brightest pixel in an object, *i.e.*, with $R > T$, $G > T$, and $B > T$, where T is a threshold (*e.g.*, point A in Fig. 12), an incorporating pixels outside the matte circle. The condition that highlight pixels must be outside the matte circle will exclude bright pixels which are not highlight. Since a highlight region may not be continuous due to some irregularities of the surface, the entire object region is scanned for any other bright pixels (*i.e.*, with $R > T$, $G > T$ and $B > T$), and the region growing process is repeated from these pixels.

A new boundary of the spectral cluster is then determined after the highlight pixels have been removed. In order to analyse the shape of the boundary, the distance of every boundary point from the matte centre is calculated as illustrated in

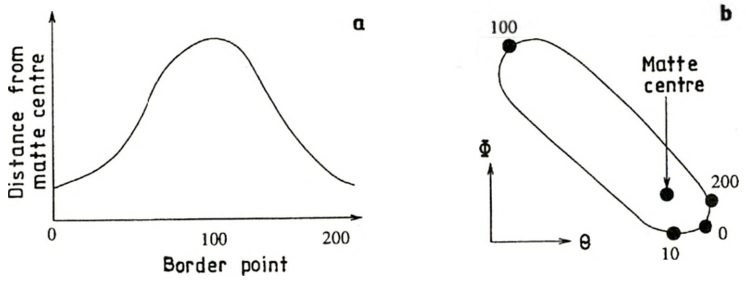

Fig. 13. Analysing the shape of the boundary (a) of the spectral cluster (b)

Fig. 13. If there is a region of interreflection then the maximum in the curve (distance from matte centre versus border point) is significant, otherwise there are only small insignificant maxima. The following four criteria have been derived experimentally using twenty test images, and are used to determine whether a maximum is significant (see also Fig. 14):

1. Width of maximum > threshold (= 5).
2. $\dfrac{\text{Height of maximum}}{\text{height of left minimum}}$ and $\dfrac{\text{maximum}}{\text{height of right minimum}}$ > threshold (= 1.3).
3. $\dfrac{\text{Height of maximum}}{\text{matte radius}}$ > threshold (= 4.5).
4. Height of maximum > threshold (= 20).

Any pixels which correspond to points within the matte circle are considered as matte pixels. They are removed so as to segment the matte region. If there are more than one maximum, indicating the presence of more than one interreflection lobes,

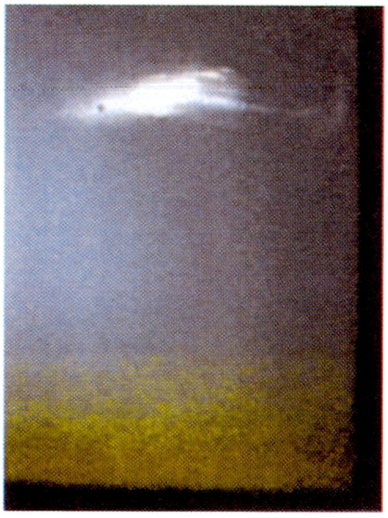

Fig. 1. Image of a green mug with interreflection

Fig. 3. Image in Fig. 1 segmented using the proposed image model

Fig. 6. Test image 1

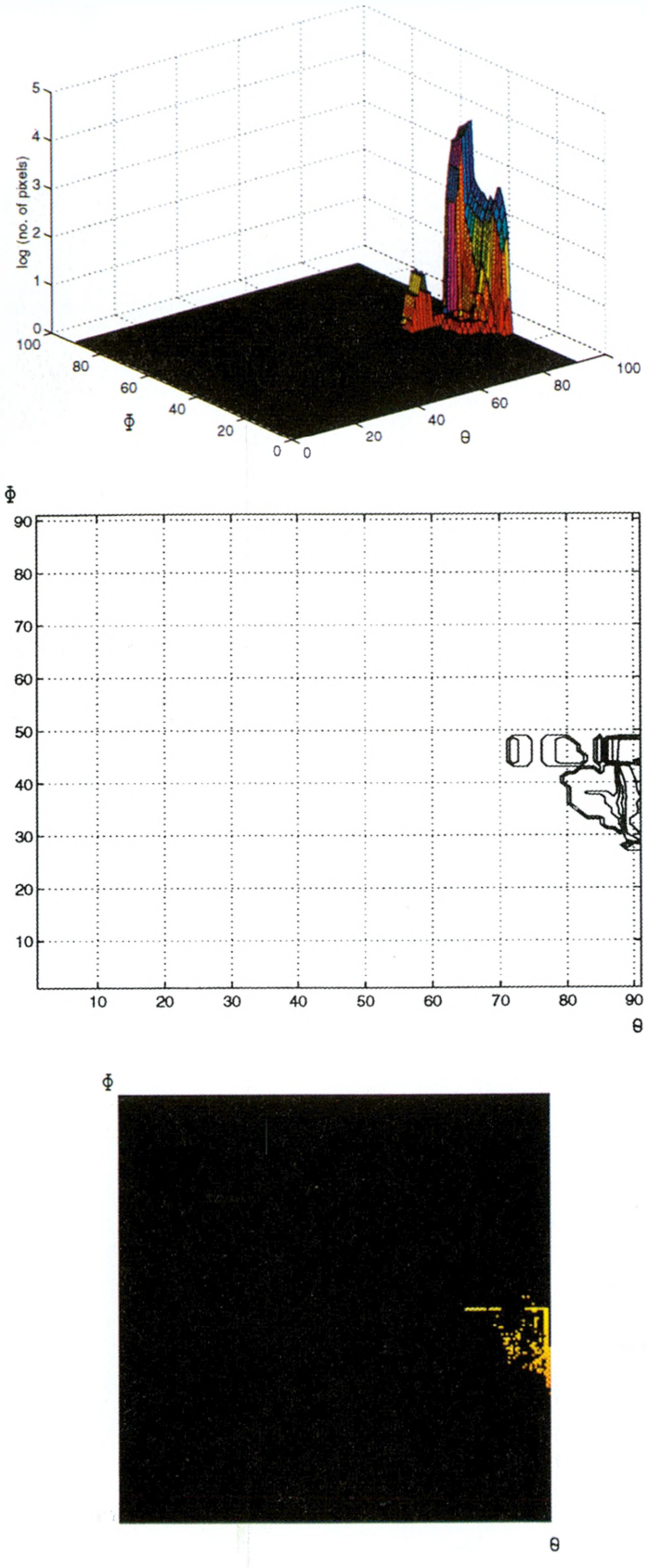

Fig. 7. Spectral cluster of the yellow cylinder in test image 1 on the $\varphi-\theta$ plane

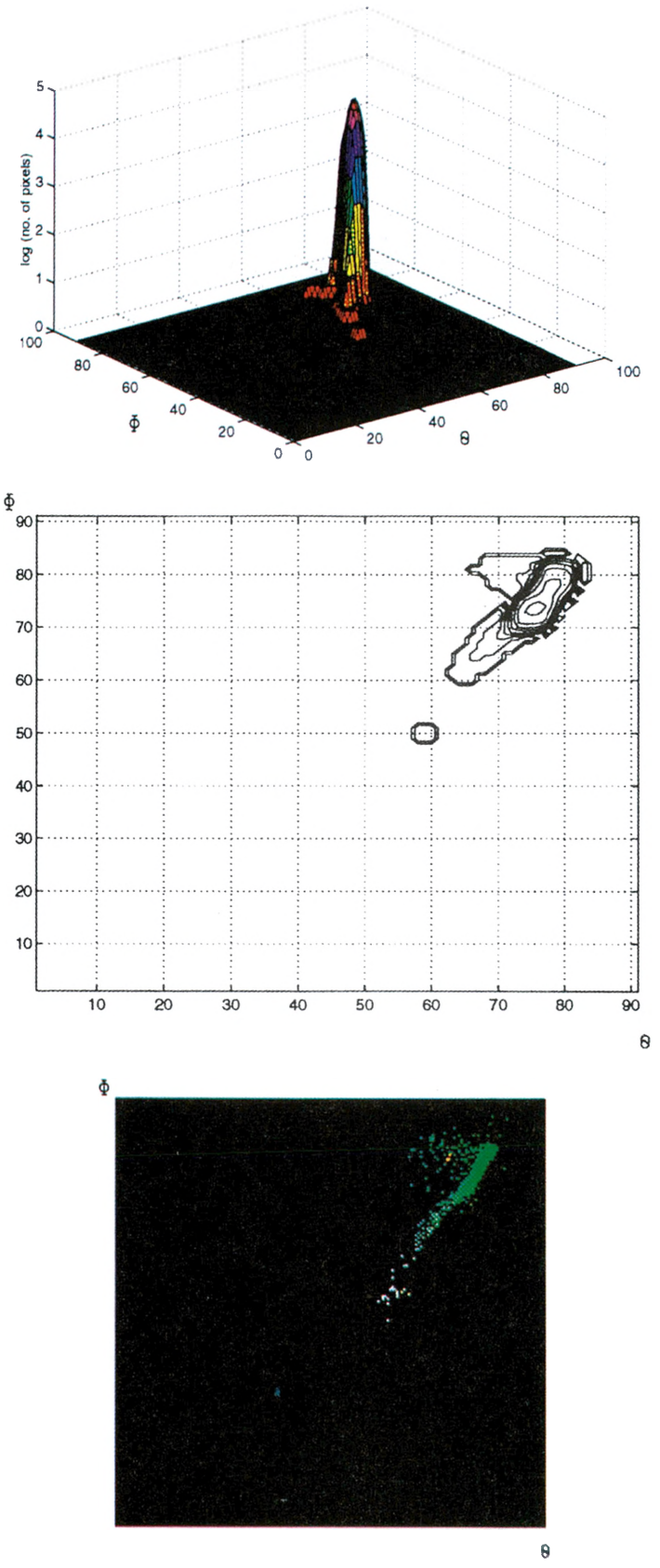

Fig. 8. Spectral cluster of the green cylinder in test image 1 on the $\varphi-\theta$ plane

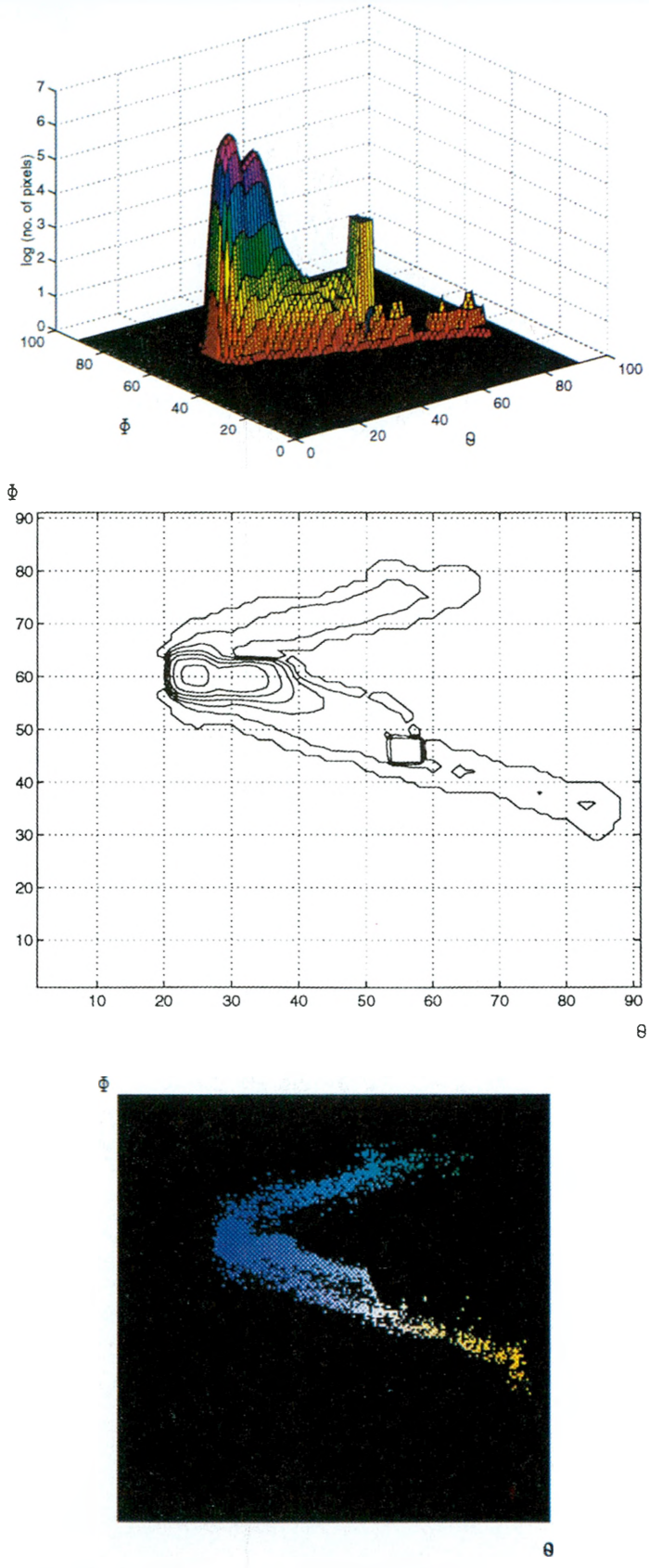

Fig. 9. Spectral cluster of the blue mug in test image 1 on the $\varphi-\theta$ plane

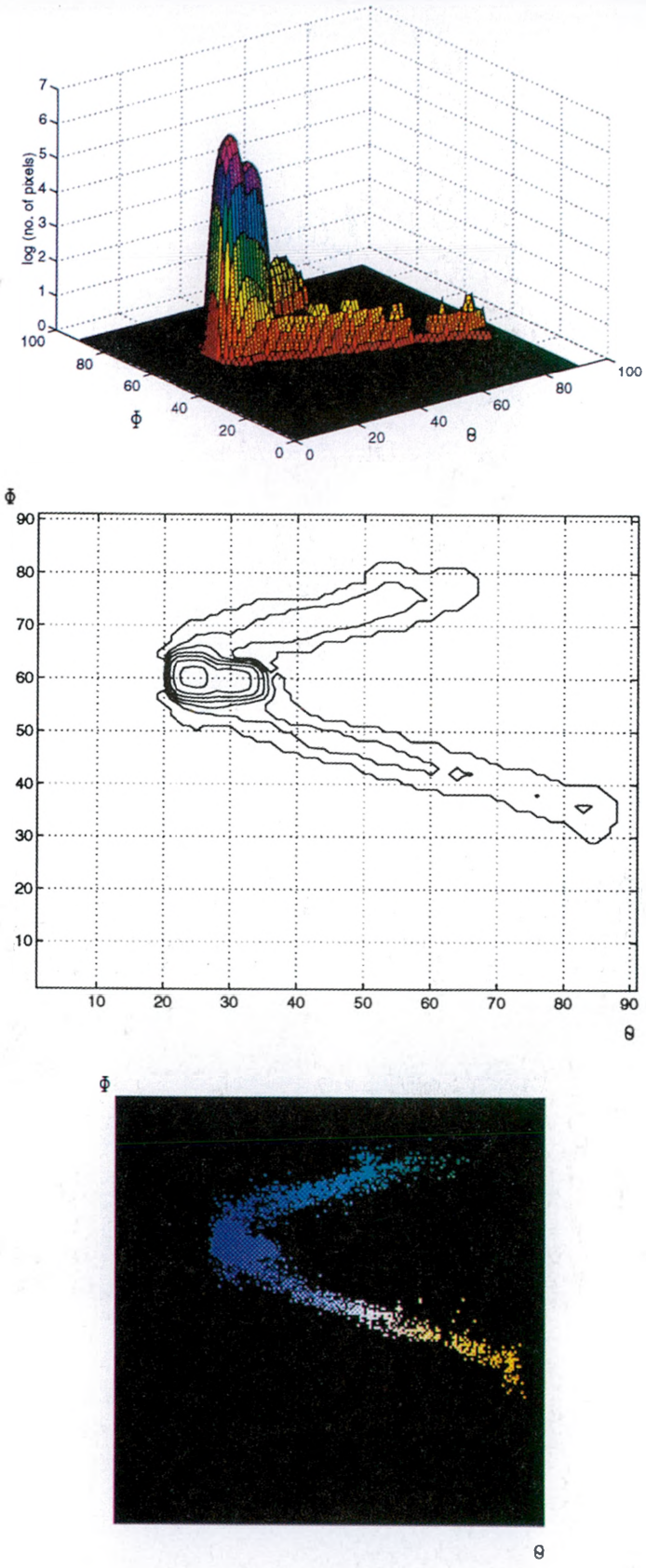

Fig. 10. Spectral cluster of the blue mug without highlight on the $\varphi-\theta$ plane

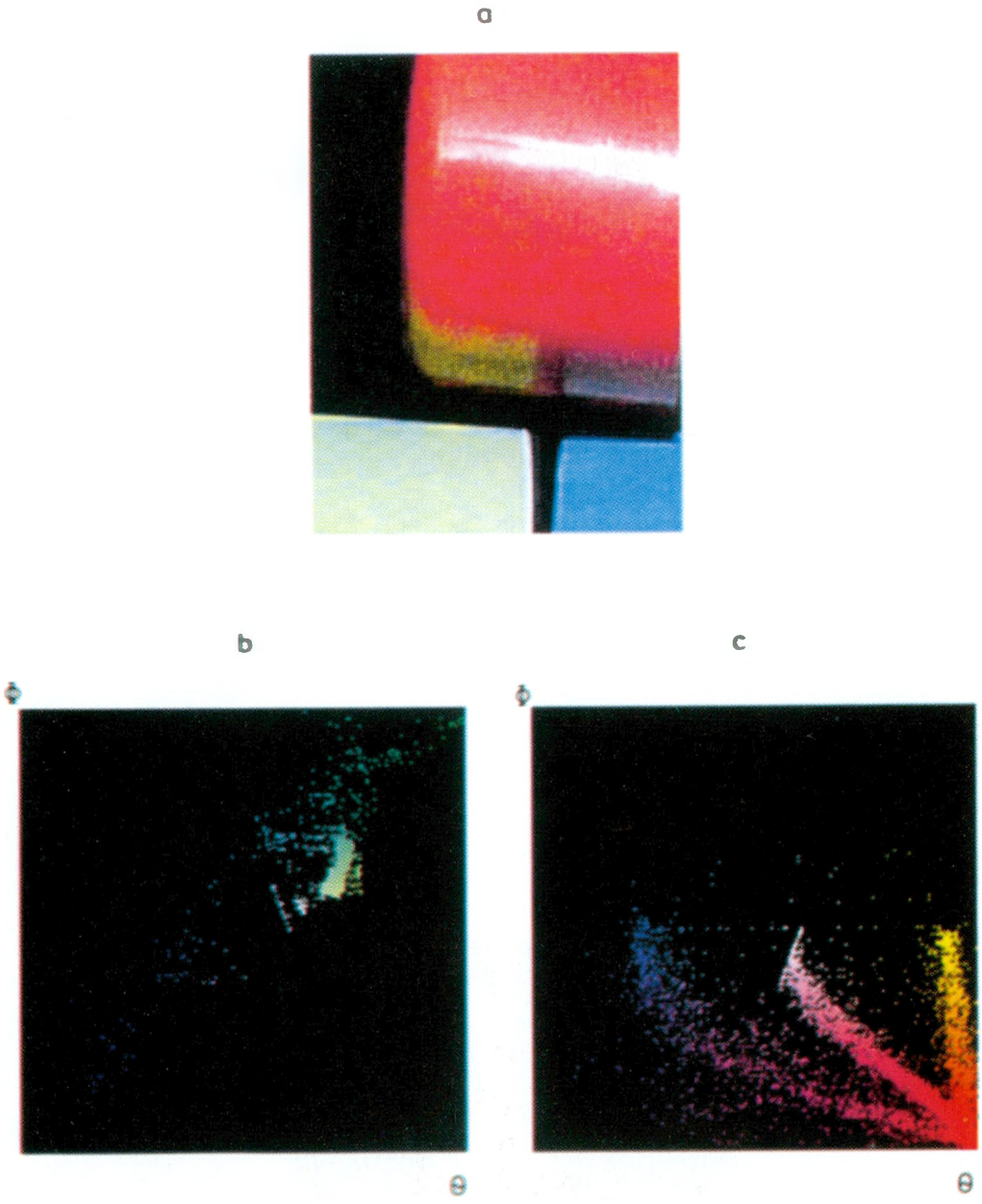

Fig. 11. Test image 2 (a), the spectral clusters of the green cylinder (b) and the red cap (c) in test image 2 on the $\varphi-\theta$ plane

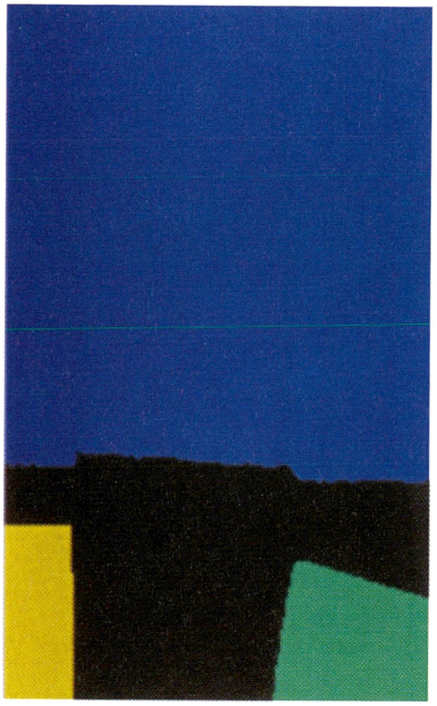

Fig. 15. Segmentation of test image 1 into background and object regions using thresholding

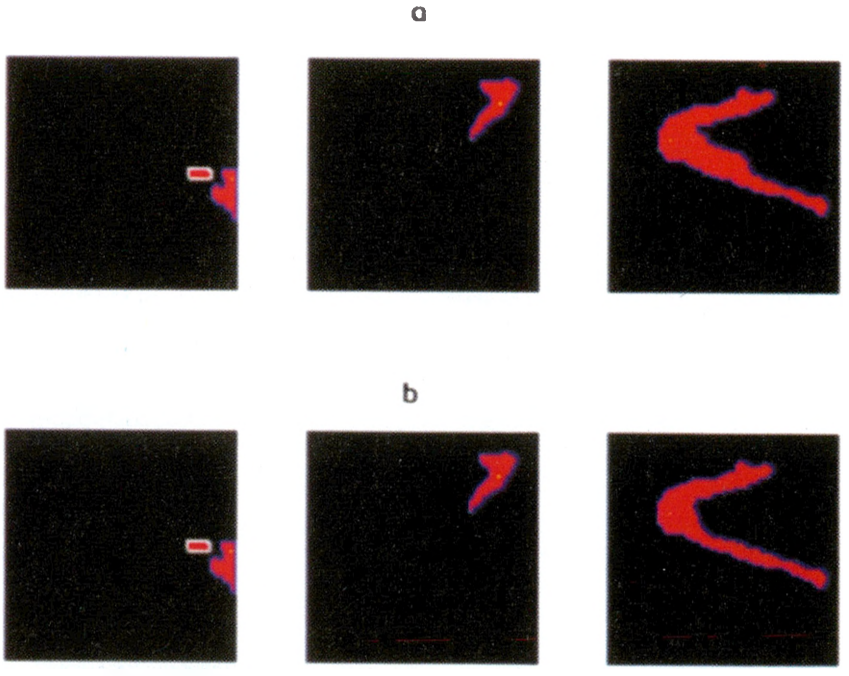

Fig. 16. Boundary of the three spectral clusters of test image 1: **a** – with highlight, **b** – without highlight

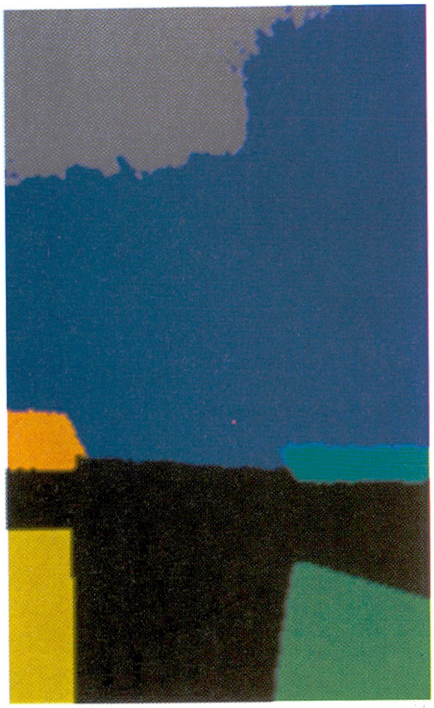

Fig. 18. Complete segmentation of test image 1

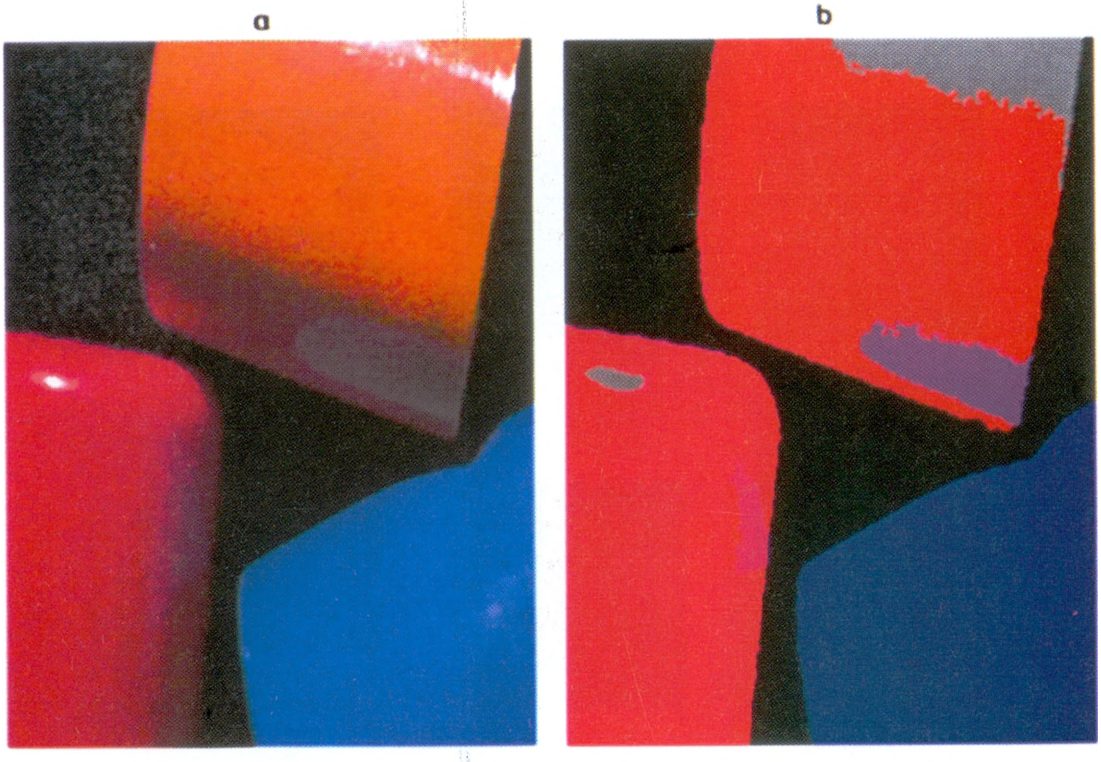

Fig. 19. Test image 3 (a) and the segmented regions (b)

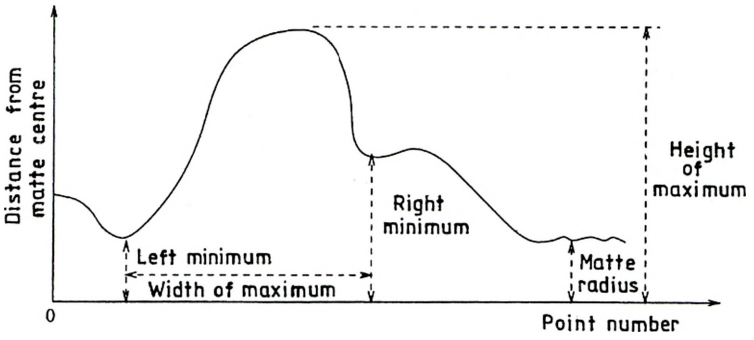

Fig. 14. Criteria for a significant maximum

then the K-means clustering algorithm is applied to the remaining points of the spectral cluster in the $\varphi-\theta$ colour space. Thus the K-means algorithm is only applied to regions of interreflection, and only if there are more than one interreflection lobes. This does not assume that the regions of interreflection have some characteristic colours. If there is a painted region on an object which is of a different hue to the object, then the region would not be identified as a region of interreflection by the proposed image segmentation algorithm. This is because there would be no connection between the spectral clusters of the region and the object in the $\varphi-\theta$ colour space. The nonmetric similarity function [11] is used as the similarity measure

$$s(x,z) = \frac{x'z}{\|x\|\,\|z\|}. \tag{14}$$

This function gives the cosine of the angle between the vectors x and z. It is maximum when x and z are oriented in the same direction with respect to the matte centre. This function is used because the cluster points are clustered along the principal axes of the interreflection lobes.

The number of clusters and the initial guess of the centres of the clusters are required when using the K-means clustering algorithm. The number of clusters to be identified by the clustering algorithm is indicated by the number of significant maxima. The initial guess of the cluster centres is the border point numbers which correspond to the peaks of the maxima. The number of clusters identified corresponds to the number of regions of interreflection in the image.

The image segmentation algorithm is summarised below.

- Segment the image into background and object regions using thresholding.
- For each object region:

1) create the histogram in the $\varphi-\theta$ colour space and determine the tallest peak, which corresponds to the matte centre,

2) determine the boundary of the spectral clusters,

3) determine the radius of the base of the matte hill,

4) remove any highlight pixels by applying a region growing process,

5) determine the boundary of the spectral cluster without any highlight,
6) analyse the shape of the boundary to determine any significant maxima,
7) remove matte points which are within the matte radius,
8) apply K-means clustering algorithm using the nonmetric similarity function if there are more than one maximum.

– Colour code the matte pixels, highlight pixels, and pixels which belong to the clusters identified by the clustering algorithm onto the original image.

5. Results

Test image 1 (Fig. 6) is used to illustrate the various stages of the proposed segmentation process. Figure 15 (see coloured inserts following page 212) shows the segmentation of the image into background and object regions using a thresholding process. The spectral clusters of the image in $\varphi - \theta$ space are shown in Figs. 7 – 10. The boundaries of the three spectral clusters are shown in Fig. 16**a** (see coloured inserts following page 212). The boundaries after the highlight pixels have been removed are shown in Fig. 16**b**. Note that only the spectral cluster of the blue mug is affected. This is because the highlight regions in the other two objects are too small to be significant. Note also that there are two boundaries in the spectral cluster of the first object (the yellow cylinder). The larger boundary is chosen to be the boundary of the matte hill.

Figure 17 (see coloured inserts following page 212) shows the distance of every boundary point from the matte centre for the three objects in test image 1. According to the criteria for a significant maximum, only the blue mug has significant maxima, indicating two regions of interreflection. Therefore, the yellow and green cylinders are entirely matte object regions, and the K-means clustering algorithm is applied to the blue mug. The results of the segmentation are shown in Fig. 18 (see coloured inserts following page 212) . The segmented regions are colour coded according to the average colour of the region. The figure shows that the detected highlight region seems much larger than what is normally considered as a highlight, *i.e.*, a clipped area. This is because a highlight region is an area which is affected by a direct illumination, and it is much larger than the clipped area.

Another image is used to test the proposed segmentation algorithm. Fig. 19**a** (see coloured inserts following page 212) shows an image with three plastic caps, two of which have a highlight and a region of interreflection. The results of the segmentation of this image are shown in Fig. 19**b**. The segmentation of both test images 1 and 3 shows that the proposed image segmentation algorithm have correctly classified the matte region, highlight regions, and regions of interreflection.

6. Conclusions

This paper proposes a reflection model based on the dichromatic reflection model which provides a means of relating the physics of light reflection to colour changes in both the image and colour spaces. It also propose the $\varphi - \theta$ colour space which

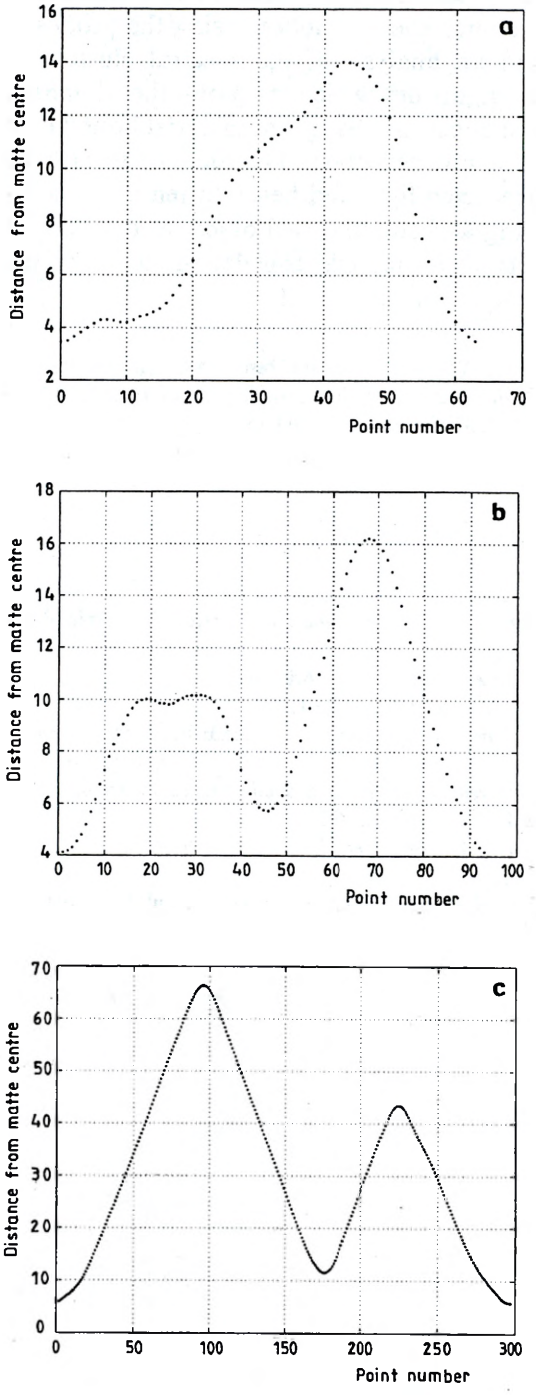

Fig. 17. Analysis of the boundary of the spectral cluster of: **a** — the yellow cylinder, **b** — the green cylinder, and **c** — the blue mug in test image 1

enables the spectral cluster of an object to be identified as consisting of a matte hill, a highlight lobe and possibly one or more interreflection lobes. Using the proposed model and the information derived from an analysis of the spectral clusters in the $\varphi - \theta$ colour space, a segmentation algorithm which employs the K-means clustering algorithm successfully distinguishes colour changes at material boundaries from changes due to shading, highlight, or interreflection. The model can also be used to determine the colour of the interreflected light and hence to remove it so as to facilitate an accurate shape-from-shading and colour-based object recognition. If the nature of the spectral clusters of objects of various shapes is determined, then the model could be used to determine the shape of an object.

Acknowledgements – The authors would like to thank NATO Collaborative Research Grants Programme (CRG 931451) for providing funds to support the international collaboration. Financial support from NSERC of Canada through grant number OGP0000370 is gratefully acknowledged.

References

[1] FUNT B. V., DREW M. S., IEEE Trans. PAMI **15** (1993), 1319.
[2] WEISSHOPF V., Sci. Am. **219** (1968), 60.
[3] SHAFER S. A., Color Res. Appl. **10** (1985), 210.
[4] EGAN W. E., HILGEMAN T. W., *Optical Properties of Inhomogeneous Material*, Academic Press, New York 1979.
[5] HUNTER R. S., *The Measurement of Appearance*, Wiley, New York 1975.
[6] TORRANCE K. E., SPARROW E. M., J. Opt. Soc. Am. **57** (1967), 1105.
[7] NAYAR S. K., IKEUCHI K., KANADE T., *Shape from interreflections*, Proc. IEEE Int. Conf. *Computer Vision* 1990, p. 2.
[8] DREW M. S., FUNT B. V., *Calculating surface reflectance using a single-bounce model of mutual reflection*, Proc. IEEE Int. Conf. *Computer Vision*, 1990, p. 393.
[9] KLINKER G. J., SHAFER S. A., KANADE T., Int. J. Computer Vision **4** (1990), 7.
[10] HEALEY G., J. Opt. Soc. Am. A **6** (1989), 920.
[11] TOU J. T., GONZALEZ R. C., *Pattern Recognition Principles*, Addison-Wesley Publ. Co., Reading, Massachusetts 1974, p. 94–95.

Received July 10, 1996